NASA TN D-1006

TECHNICAL NOTE

D-1006

EFFECT OF GEOMETRIC PARAMETERS ON THE STATIC PERFORMANCE OF AN ANNULAR NOZZLE WITH A CONCAVE CENTRAL BASE

By Charles E. Mercer and Albert J. Simonson

Langley Research Center
Langley Air Force Base, Va.

NATIONAL AERONAUTICS AND SPACE ADMINISTRATION

WASHINGTON February 1962

NATIONAL AERONAUTICS AND SPACE ADMINISTRATION

TECHNICAL NOTE D-1006

EFFECT OF GEOMETRIC PARAMETERS ON THE STATIC PERFORMANCE OF AN ANNULAR NOZZLE WITH A CONCAVE CENTRAL BASE

By Charles E. Mercer and Albert J. Simonson

SUMMARY

An experimental investigation of annular convergent nozzles with concave central bases has been conducted in which the effects of variation in the ratio of annulus-gap width to base radius and the ratio of annulus-gap width to base depth were examined. Thrust performance comparable to that of a conventional convergent nozzle was obtained for those configurations in which the ratio of annulus-gap width to base radius was largest, that is, approximately 0.25. In general, increasing the base depth by extending the turning lip improved thrust performance and increased pressures on the base.

INTRODUCTION

Studies of jet efflux, in which three or more parallel nozzles were clustered in close proximity to each other, have disclosed that interference between the individual jets can result in reversal of a portion of that flow confined between the adjacent jet boundaries. In references 1 and 2, studies of the manner in which this flow reversal affects conditions on a missile base indicate that pressures over the base are increased under certain conditions. An attempt to utilize this base pressure rise through the use of an annular convergent nozzle with a concave central base was reported in reference 3. The thrust ratio obtained was comparable to that of conventional convergent nozzles operating at low pressure ratios, but did not indicate the underexpansion losses characteristic of convergent nozzles at high pressure ratios. In an attempt to exploit these favorable results, three series of nozzles were tested to determine the effect of geometric parameters on the nozzle performance and the results are reported herein. The first series of nozzles (series A) used in the present investigation were designed with turning lips having small radii of curvature in order to avoid excessive boattail drag and internal losses. However, since series A nozzles exhibited poor static performance, other nozzles (series B and C) were tested. These nozzles closely resembled the exploratory nozzle of reference 3, but they were designed to vary some of the geometric parameters which affect nozzle performance.

The purpose of the present investigation was to determine the effect of some geometric parameters on the static performance of an annular nozzle with a concave central base. The main points of inquiry were to determine the effects of g/R and g/l on both the general pressure level and the distribution of pressures over the central base and to determine the effects of these ratios on the variation of overall thrust performance with jet total-pressure ratio. The test was conducted in the jet-exit test stand of the Langley 16-foot transonic tunnel.

SYMBOLS

F measured thrust, lb

F_b base thrust, $2\pi \int_0^R \left(p_b - p_a\right) r \, dr$, lb

F_i ideal thrust for complete isentropic expansion of primary flow, $w\sqrt{\frac{2R}{g} \frac{\gamma}{\gamma - 1} T_{t,j} \left[1 - \left(\frac{p_a}{p_{t,j}}\right)^{\frac{\gamma-1}{\gamma}}\right]}$, lb

g gravitational acceleration, ft/sec^2; or annulus-gap width, in.

l distance from nozzle-exit plane to concave base, in. (see fig. 1)

p static pressure, lb/sq ft

p_t total pressure, lb/sq ft

$p_{t,j}/p_a$ ratio of primary jet total pressure to ambient static pressure

R gas constant (69.89 for 90 percent H_2O_2 products at 1,364° F), ft/°R; or base radius, in.

r radial distance from base center to pressure orifice, in.

T_t total temperature, °R

w	measured weight flow, lb/sec
γ	ratio of specific heats (1.266 for 90 percent H_2O_2 products at 1,364° F)
θ	design turning-lip angle, deg (see fig. 1)
ϕ	actual discharge-convergence angle at the jet exit, measured from center line, deg

Subscripts:

a	ambient (atmospheric)
b	base
j	jet

APPARATUS AND METHODS

The present investigation was conducted at the jet-exit test stand of the Langley 16-foot transonic tunnel. Three series of convergent nozzles with concave central bases which formed annular exits were tested. Series A (fig. 1) consisted of models with a short nozzle-lip overhang, a constant ratio of annulus gap to base radius ($g/R \approx 0.15$), and nozzle turning-lip angles varying from 15° to 60°. Series B and C (fig. 1) had constant turning-lip angles of 15° and 30°, respectively, and varying ratios of annulus gap to base radius and annulus gap to base depth. A hydrogen peroxide turbojet-engine simulator of the type described in reference 4 was used to produce a hot-jet exhaust. Sketches of the configurations are presented in figure 1, and photographs of two of the models tested are presented in figure 2.

The instrumentation included a one-component strain-gage thrust balance, a total-pressure probe and a total-temperature probe located in the tailpipe, static-pressure orifices on the external portion of the afterbody and on the concave central base located 45° in a clockwise direction from the top, and an impeller-type electronic flowmeter. The pressures were measured with electrical pressure transducers with outputs transmitted to and recorded by an automatic digitizer system. The thrust-balance and flowmeter outputs were also recorded by this system. The jet stagnation temperature was measured with a pen-trace self-balancing potentiometer. The pressure and forces were converted to absolute units and ratios by machine computations.

The estimated accuracy of the pressure measurements is ±2 percent. Thrust measurements are estimated to be accurate within ±4 pounds of thrust, and measured weight flow is estimated to be accurate within ±0.02 pound per second.

RESULTS AND DISCUSSION

The results of the measurements of base pressures, flow-visualization studies, static thrust, and weight flow for the various configurations tested are presented in figures 3 to 11. Pressures on the external portion of the afterbody were found to have no measurable effect on thrust and are, therefore, not presented.

L
1
6
4
6

Base Pressures

Figure 3 presents the base pressure distributions for the series A nozzles, in which the ratios of annulus gap to base radius g/R were held constant at approximately 0.15. For these nozzles, with the exception of configuration IV, the pressures on the concave central base generally were less than ambient. This suggests that aspiration was the predominant phenomenon for all these configurations as evidenced by the poor thrust performance shown subsequently. The flow-visualization photographs in figure 4 substantiate this, since it can be seen that for series A the flow boundaries curved toward the axis of symmetry. Furthermore, the actual discharge-convergence angle immediately behind the jet exit ϕ was measured as about 18° for this configuration, whereas the design turning-lip angle θ was 30°. From figures 3 and 4 it was concluded that the short turning lips of these nozzles were not sufficiently effective in converging the flow. (See ref. 5.) The poor performance of the series A nozzles may be attributed to several causes. Primarily, the low values of actual flow-convergence angles resulted in an extensive surface of contact between the annular jet and the fluid contained in the base region, a condition favorable to mixing of the two fluids. Furthermore, the ineffectiveness of the turning lips may have permitted a peripherally nonuniform convergence of the flow with accompanying turbulence. Both these conditions could result in aspiration of the base region.

The base pressures for the series B nozzles ($\theta = 15^\circ$) as presented in figure 5 show similar effects of aspiration, and for these configurations the low values of design turning-lip angle contributed to establishing similar mixing conditions. For configurations in which the turning lip extended well beyond the base (low g/l), for example, configuration VI, base pressures exceeded ambient pressure and increased with increasing jet total-pressure ratio.

Figure 6 shows the base pressure distributions for the series C nozzles. As with the series B nozzles, with other factors similar, extending the turning lip appears to have increased base pressures. In addition, nozzles with large ratios of annulus gap to base radius g/R exhibited higher base pressures for the same values of jet total-pressure ratio and g/l. It is evident that for the series C nozzles the effects on base pressure which resulted from redirecting the jet flow to an axial direction were more significant than were the effects of aspiration.

The base pressure distributions for several of the configurations (III, IV, VII, and Xa) indicated higher pressures at the center of the base and at the outer edge, which suggests the existence of a vortex-ring type of flow contained between the converging annular jet and the central base, as noted in reference 3. However, consideration of the change in axial fluid momentum between the exit and a point in the flow after axial redirection does not require that a ring vortex flow be a fundamental mechanism by which flow redirection and base thrust are attained. If the static pressure in the confined base region is sufficiently high, the converging flow is redirected axially in a gradual manner. If, however, the base pressure is not sufficiently high to redirect the flow (as in initiating nozzle flow), converging streamlines meet at finite angles. For subsonic inviscid flow, a backflow along the axis toward the base is required in order to satisfy the axial momentum relation; thus the pressure of confined gases in the base region is raised until the backflow is no longer necessary. If the converging flow is entirely supersonic, viscosity becomes a dominant influence on the backflow and base pressurization. This aspect is discussed in greater detail in reference 1 in connection with jet interference. A ring-vortex flow can exist when the gases in the base region are entrained by the converging jet flow because in such cases the gases in the base region are not truly confined.

Base Thrust

Base pressures for all configurations were integrated over the base area in order to obtain values of base thrust as indicated in figures 7 to 9. These figures show that generally when the base thrust was positive, it increased with jet total-pressure ratio as was to be expected from the results of reference 3. Furthermore, the variation of base thrust with jet total-pressure ratio is of increasing slope where base thrust is positive. This increasing slope with increasing pressure ratio is most pronounced for configurations having long lip overhangs (low g/l). The increasing ratio of base thrust to jet thrust for these cases may be attributed to the fact that, for large values of l, the flow issuing from the annulus had only one solid boundary,

which was the lip overhang. Thus, for high jet total-pressure ratios $\left(\frac{p_{t,j}}{p_a} > 1.81 \frac{p_b}{p_a}\right)$ the jet was permitted to expand toward the axis of symmetry, and the actual convergence of the flow and consequently the base pressures increased. Variations in the extent of aspiration and external flow expansion would influence the nonlinearity of the base-thrust curve for all configurations.

Nozzle Performance

The variations of measured thrust, ideal isentropic thrust, and thrust ratio with jet total-pressure ratio are presented in figures 7 to 9 for the various configurations. The performance of the series A nozzles is shown to be poor, primarily as a result of base aspiration. The effect of lip angle could not be determined for these nozzles inasmuch as the lip was not of a length sufficient to converge the jet streamlines toward the axis of symmetry.

Losses were generally small for the series B and C nozzles in which a smoothly contoured base and an extended lip overhang were employed. These configurations tend to show that for increasing jet total-pressure ratios the thrust ratios do not exhibit the decrease which is characteristic of conventional convergent nozzles due to incomplete expansion of the nozzle flow. (See ref. 6.)

For turning-lip angles of 15° and 30° and various jet total-pressure ratios, the effects on nozzle performance of g/R and g/l are shown in figures 10 and 11, respectively. For nozzles with either turning-lip angle, the thrust ratio was highest when the ratio of annulus gap to base radius g/R was near the maximum tested (fig. 10). The ratio of annulus gap to base depth g/l had little effect on the 15° nozzles, but the 30° nozzles showed a distinct improvement as the base depth was increased. Although the nozzles with the extended lips showed good performance for static conditions, the increase in boattail area would undoubtedly incur higher external drag in an airstream.

Although thrust performance was best for nozzles with high g/R ratios, in practice those nozzles with lower g/R ratios may be more desirable. As g/R increases, the annular nozzle configuration approaches that of a conventional convergent nozzle with no central base ($g/R = \infty$) and, thus, the advantages of the annular nozzle over the conventional convergent nozzle as stated in reference 3 become less significant. There is evidence, however, that it may be possible to improve markedly the performance of annular nozzles with low values of g/R by reducing the aspiration effect, that is, mixing at the interface

between the annular jet and the fluid contained in the base region. Reference 7, for example, shows that the divergence of a jet mixing region is diminished if the Mach number of the jet is increased relative to the Mach number of the surrounding fluid for all the degrees of expansion that were investigated. The possibility then exists that for an annular jet flow at high Mach number (perhaps partly expanded within a convergent-divergent annulus gap), thrust performance could be improved especially for nozzles with the low value of g/R and/or small lip angles θ, that is, with extensive surfaces of contact between the annular jet and the pressurized gas in the base region.

CONCLUDING REMARKS

An experimental investigation of annular convergent nozzles with concave central bases has been conducted in which the effects of variation in annulus-gap width and base depth were examined. The highest thrust ratios were obtained from those configurations in which the ratio of annulus gap to base radius was greatest. However, unreasonably large annulus gaps were unnecessary, since thrust ratios of about 97 to 99 percent of ideal were obtained from configurations for which the ratio of annulus-gap width to base radius was about 0.25. In general, increasing the base depth or extending the turning lip improved thrust performance and increased pressures on the base.

Langley Research Center,
National Aeronautics and Space Administration,
Langley Air Force Base, Va., October 24, 1961.

REFERENCES

1. Goethert, B. H.: Base Flow Characteristics of Missiles With Cluster-Rocket Exhausts. Aero/Space Eng., vol. 20, no. 3, Mar. 1961, pp. 28-29, 108-117.

2. Scott, William R., and Slocumb, Travis H., Jr.: Jet Effects on the Base Pressure of a Cylindrical Afterbody With Multiple-Jet Exits. NASA MEMO 3-10-59L, 1959.

3. Corson, Blake W., Jr., and Mercer, Charles E.: Static Thrust of An Annular Nozzle With A Concave Central Base. NASA TN D-418, 1960.

4. Runckel, Jack F., and Swihart, John M.: A Hydrogen Peroxide Hot-Jet Simulator for Wind-Tunnel Tests of Turbojet-Exit Models. NASA MEMO 1-10-59L, 1959.

5. Krull, H. George, and Beale, William T.: Effect of Outer-Shell Design on Performance Characteristics of Convergent-Plug Exhaust Nozzles. NACA RM E54K22, 1955.

6. Mihaloew, James R., and Stofan, Andrew J.: Internal-Performance Evaluation of a Two-Position Divergent Shroud Ejector. NASA TN D-762, 1961.

7. Pai, S. I., and Cary, B. B., Jr.: Two Dimensional Jet Mixing of Supersonic Flow. 50 Jahre Grenzschichtforschung, H. Görtler and W. Tollmien, eds., Friedr. Vieweg & Sohn (Braunschweig), 1955, pp. 71-79.

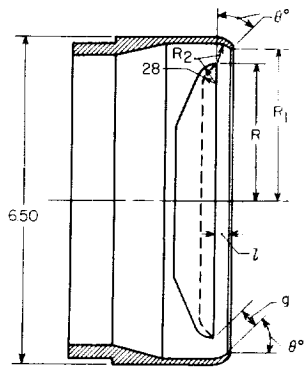

Series A

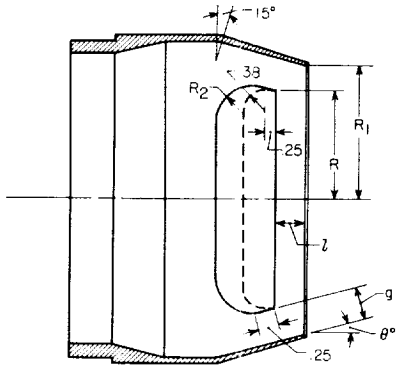

Series B

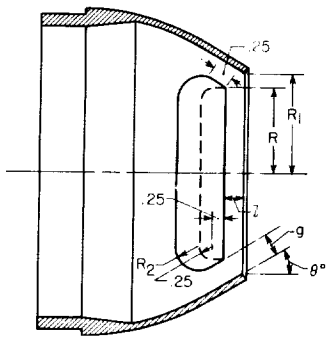

Series C

Nozzle Parameters								
Series A								
Config.	θ, deg	R	R_1	R_2	g	l	g/R	g/l
I	15	2.71	3.11	0.41	0.41	0.11	0.15	3.73
II	30	2.71	3.07	.41	.41	.21	.15	1.95
III	45	2.71	3.00	.42	.42	.30	.16	1.40
IV	60	2.70	2.91	.42	.42	.36	.16	1.17
Series B								
V	15	2.16	2.64	0.75	0.52	0.13	0.24	4.00
VI	15	2.16	2.64	.75	.63	.61	.29	1.03
VI(a)	15	2.16	2.72	.75	.63	.37	.29	1.70
VI(b)	15	2.16	2.77	.75	.63	.17	.29	3.71
Series C								
VII	30	2.00	2.00	0.55	0.22	0.44	0.11	0.50
VIII	30	2.00	2.00	.55	.37	.74	.19	.50
VIII(a)	30	2.00	2.33	.55	.37	.14	.19	2.64
IX	30	1.70	2.00	.47	.36	.20	.21	1.80
X	30	2.00	2.00	.55	.47	.94	.24	.50
X(a)	30	2.00	2.33	.55	.47	.34	.24	1.38
X(b)	30	2.00	2.39	.55	.47	.25	.24	1.88
XI	30	1.70	2.00	.47	.49	.36	.29	1.36
XII	30	1.70	2.00	.47	.54	.56	.32	.96

Pressure Orifice Locations On Concave Base					
Config.	r	r/R	Config.	r	r/R
I and II	0	0	V and VI	0	0
	.84	.31		.53	.25
	1.69	62		1.05	.49
	2.53	.93		1.58	.73
	2.65	98		2.11	.98
III and IV	0	0	IX, XI, and XII	0	0
	.84	.31		.84	.49
	1.68	.62		1.68	.99
	2.52	.93	VII, VIII and X	0	0
	2.64	98		.98	.49
				1.95	.98

Figure 1.- Nozzle geometric parameters. (All linear dimensions are in inches.)

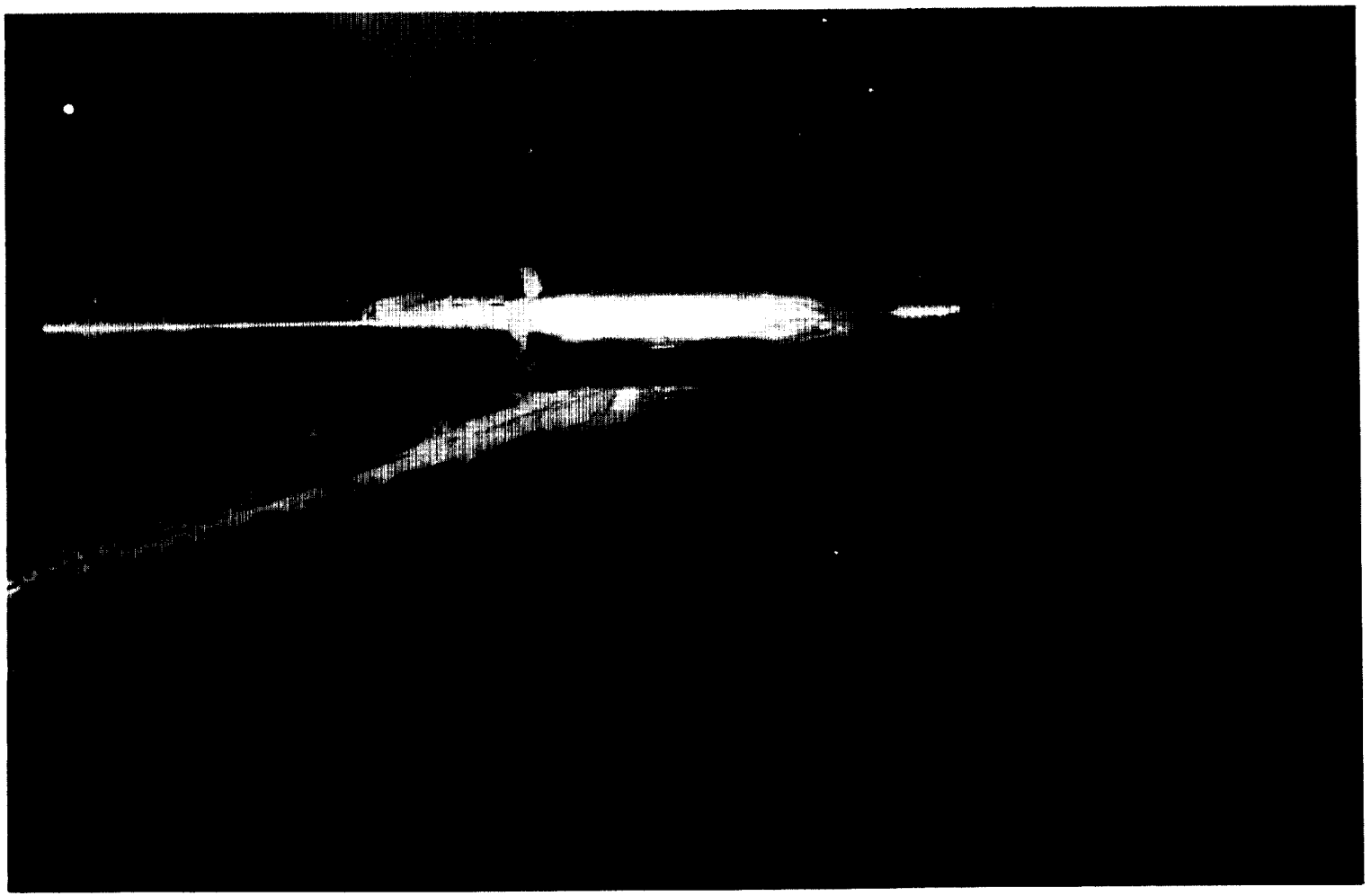

(a) Configuration II. L-60-459

Figure 2.- Photographs of models.

Three-quarter rear view

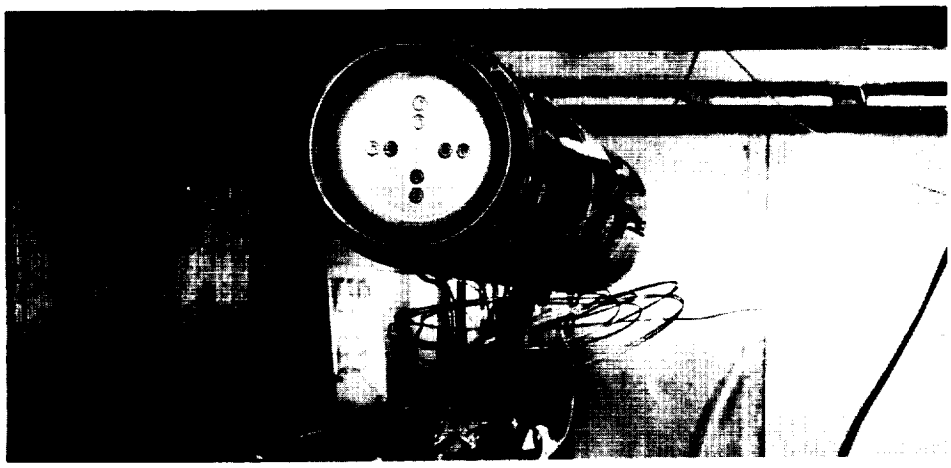

Rear view

(b) Configuration VI. L-61-5123

Figure 2.- Continued.

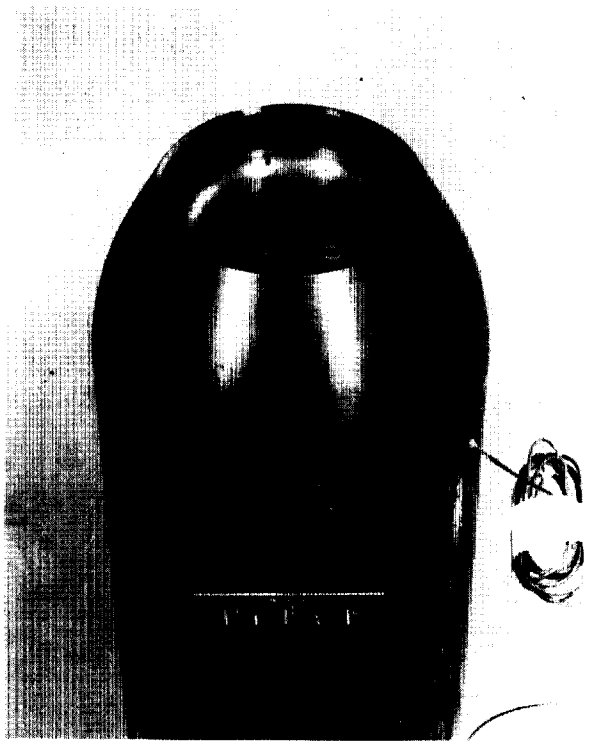

Three-quarter rear view

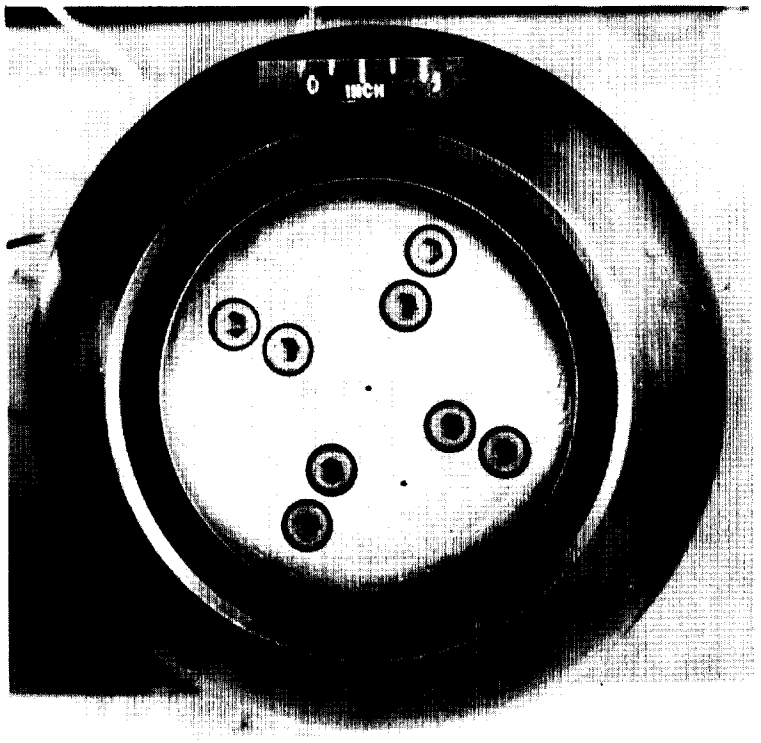

Rear view

(c) Configuration XI. L-61-5124

Figure 2.- Concluded.

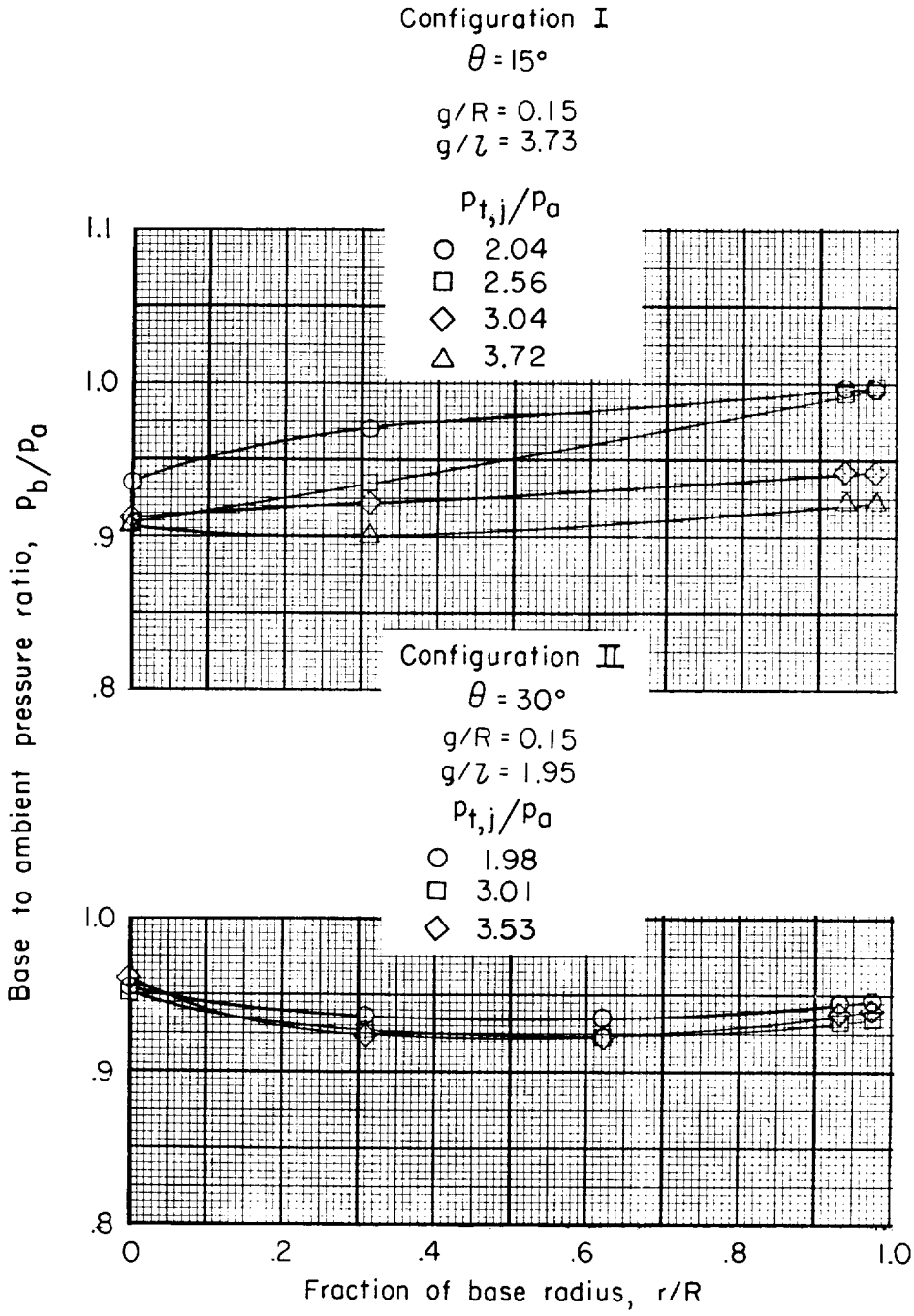

(a) Configurations I and II.

Figure 3.- Pressure distributions on concave central base of series A nozzles for various jet total-pressure ratios.

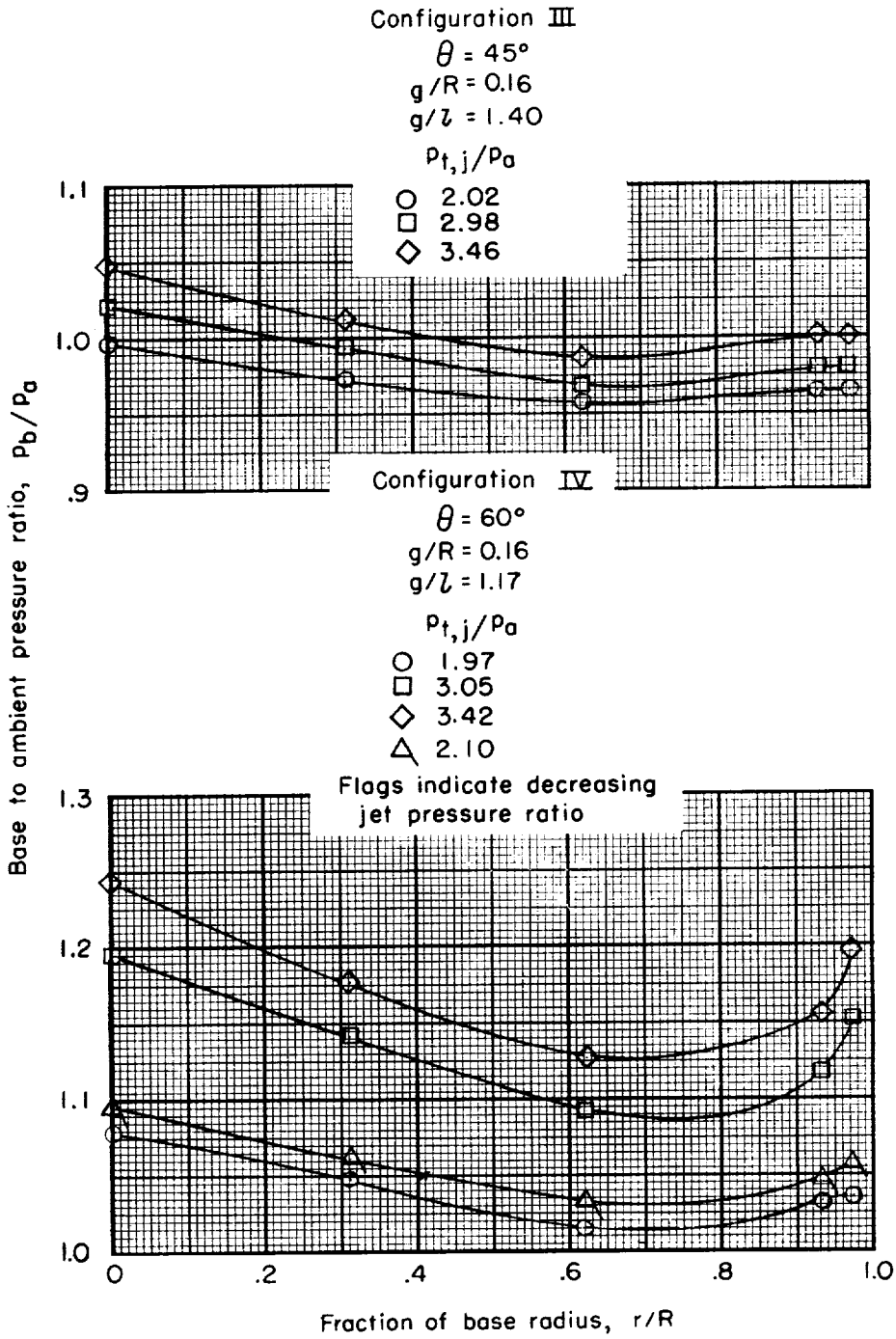

(b) Configurations III and IV.

Figure 3.- Concluded.

(a) Right side view. L-60-365

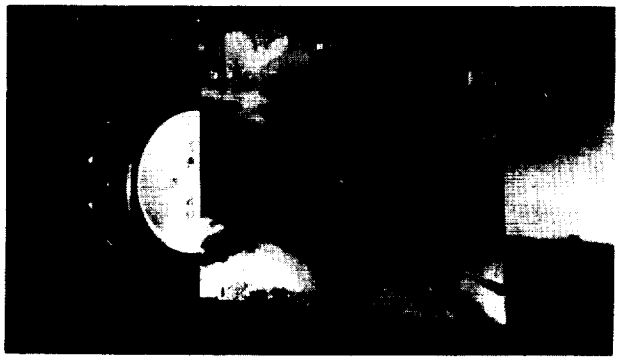

(b) Three-quarter rear view. L-60-363

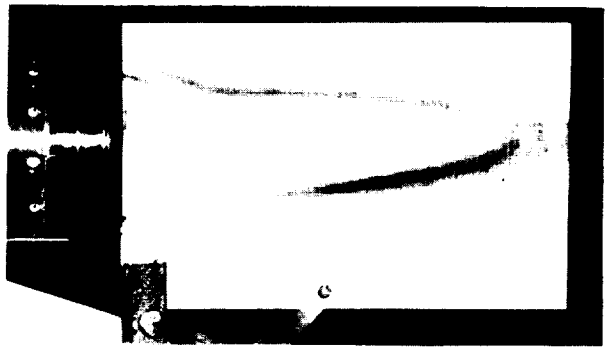

(c) Left side view. L-60-367

Figure 4.- Flow boundaries created by nozzle of configuration II exhausting over a stainless-steel flat plate for a jet total-pressure ratio of 2.0.

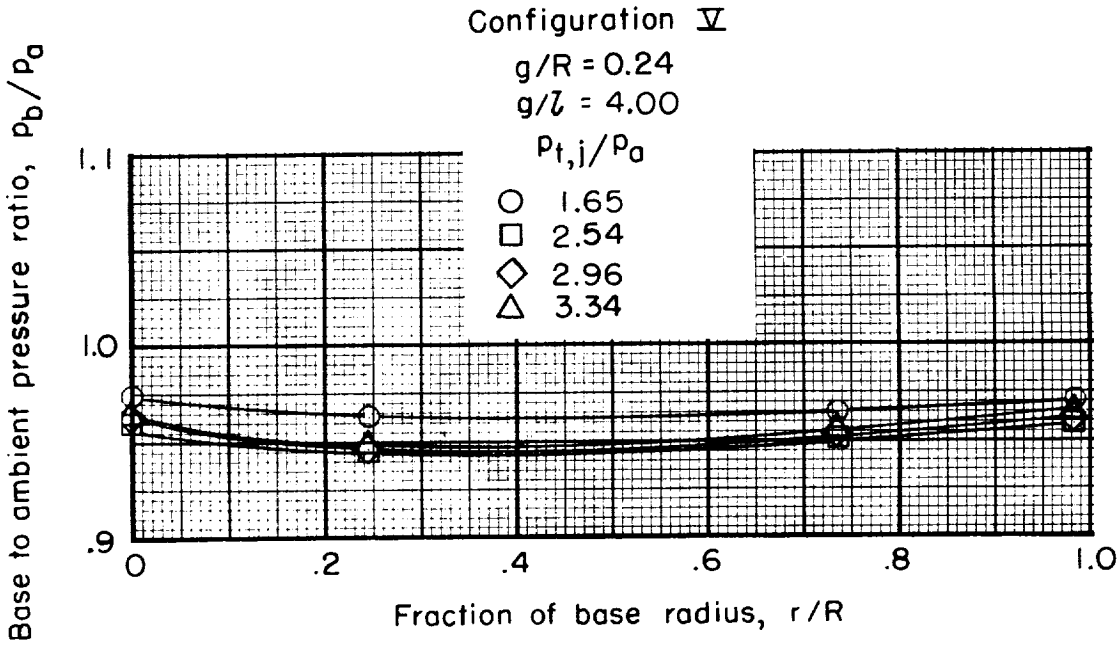

(a) Configuration V.

Figure 5.- Pressure distributions on concave central base of series B nozzles for various jet total-pressure ratios. $\theta = 15^{\circ}$.

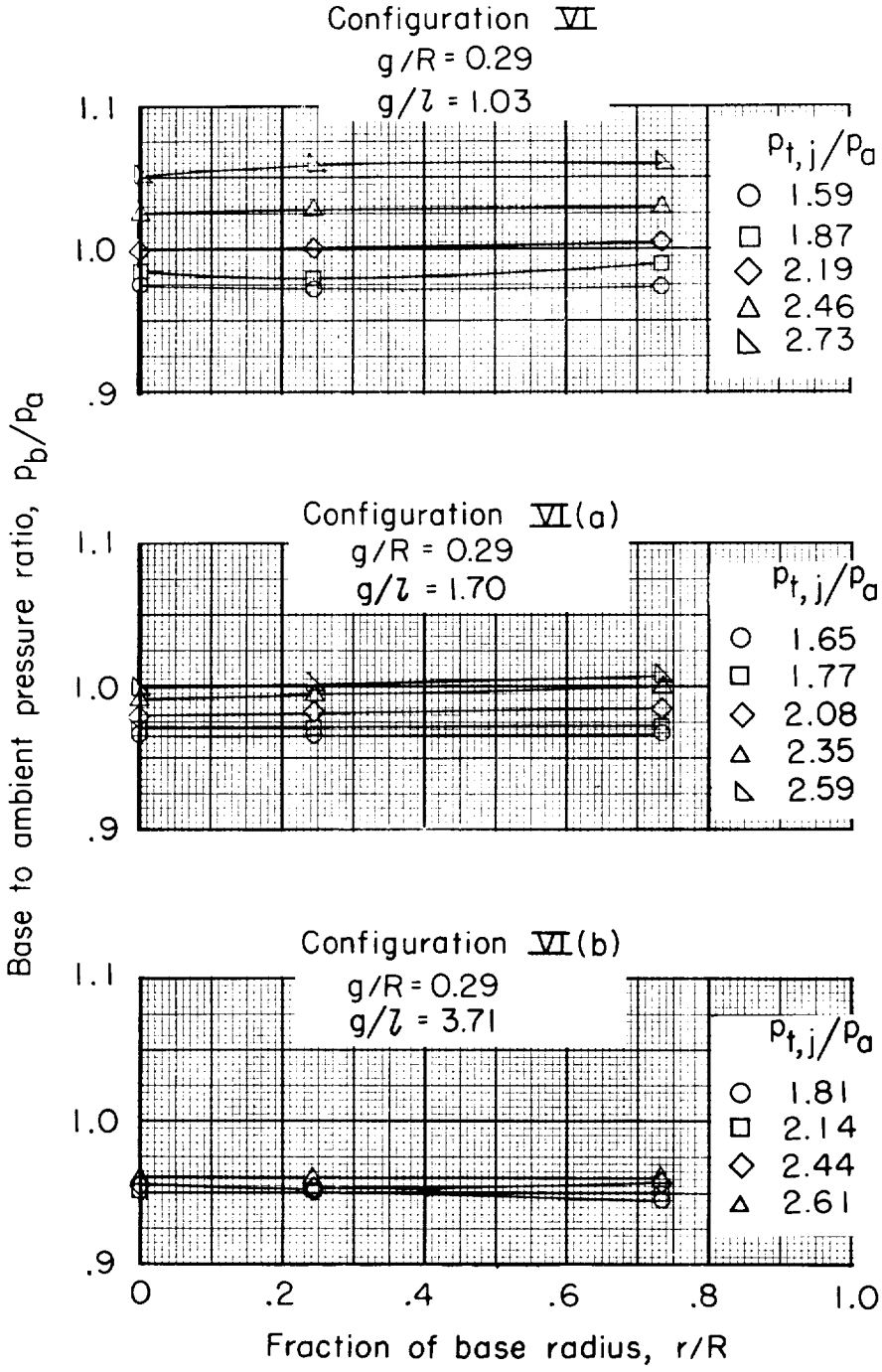

(b) Configuration VI.

Figure 5.- Concluded.

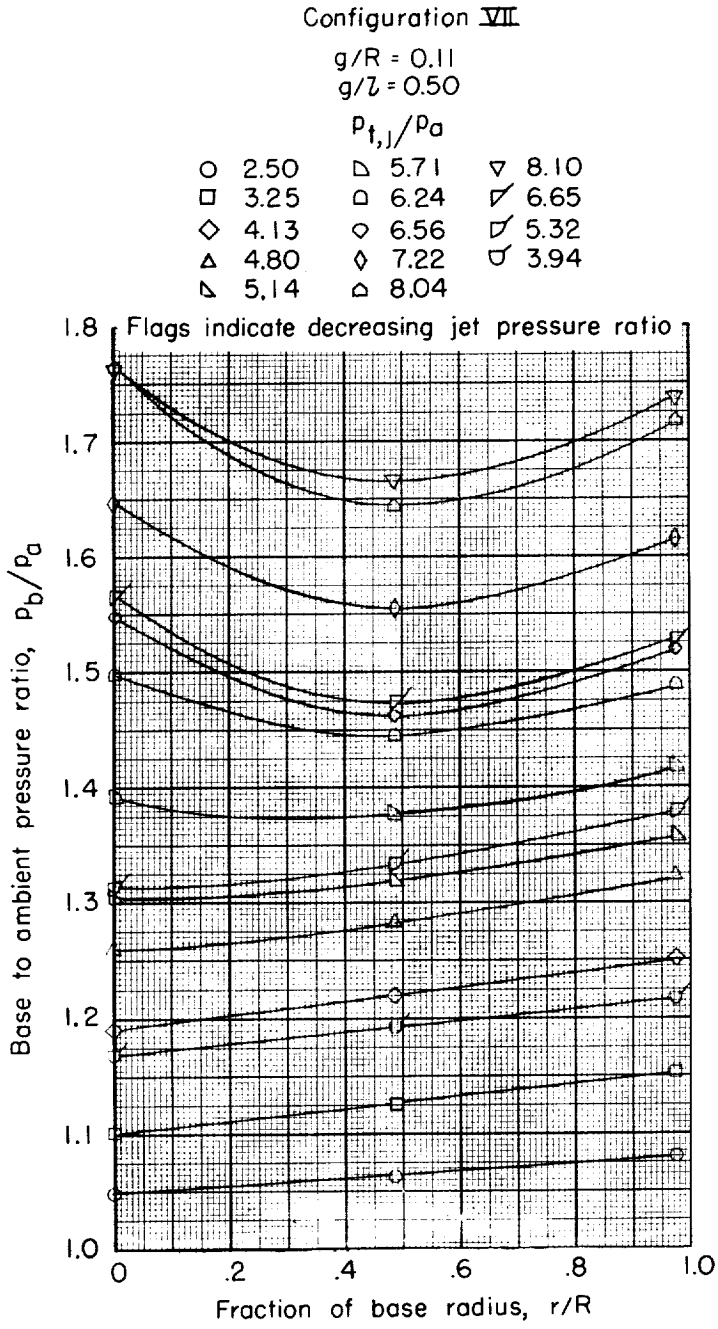

(a) Configuration VII.

Figure 6.- Concave central base pressure distributions of series C nozzles for various jet total-pressure ratios. $\theta = 30^\circ$.

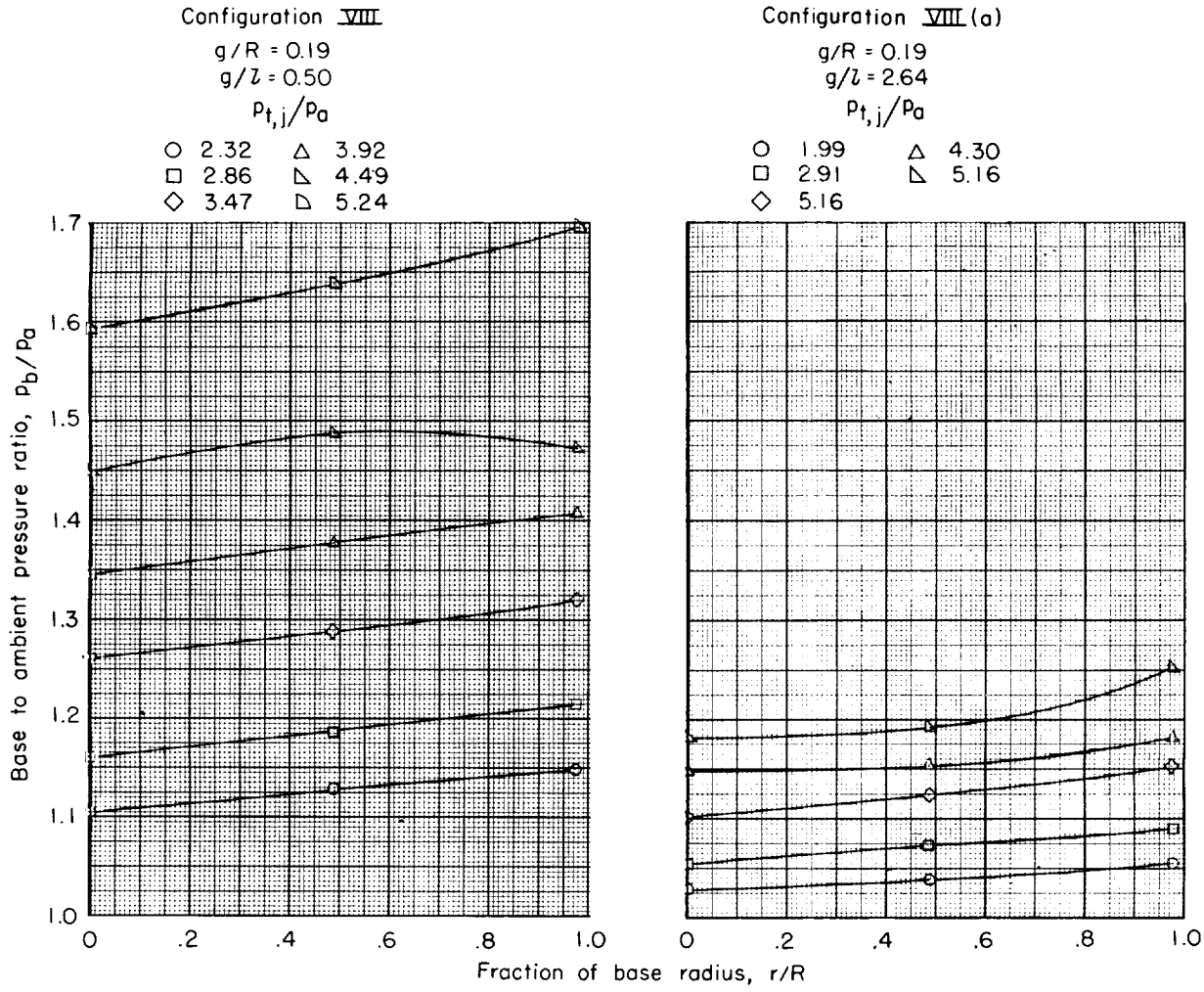

(b) Configuration VIII.

Figure 6.- Continued.

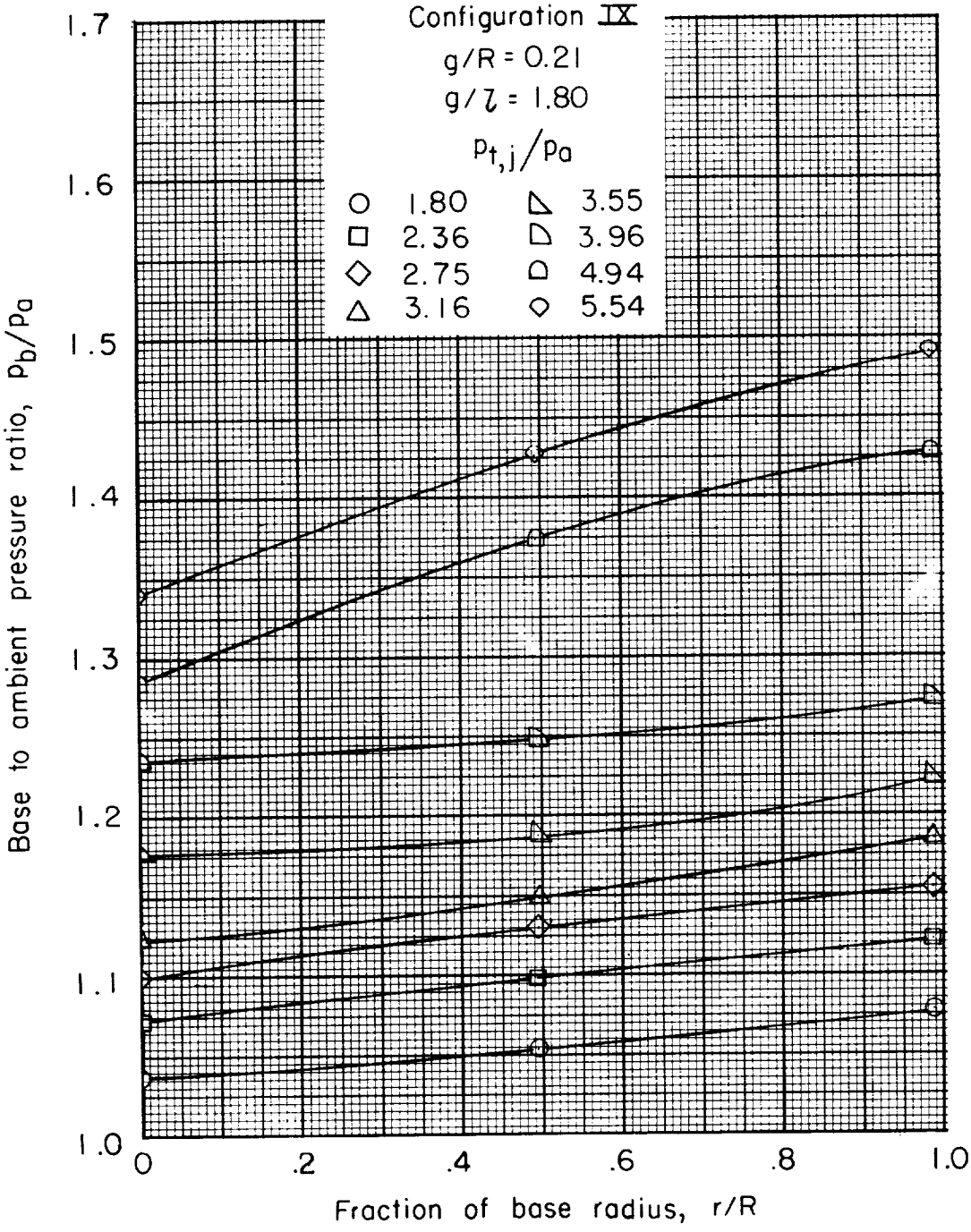

(c) Configuration IX.

Figure 6.- Continued.

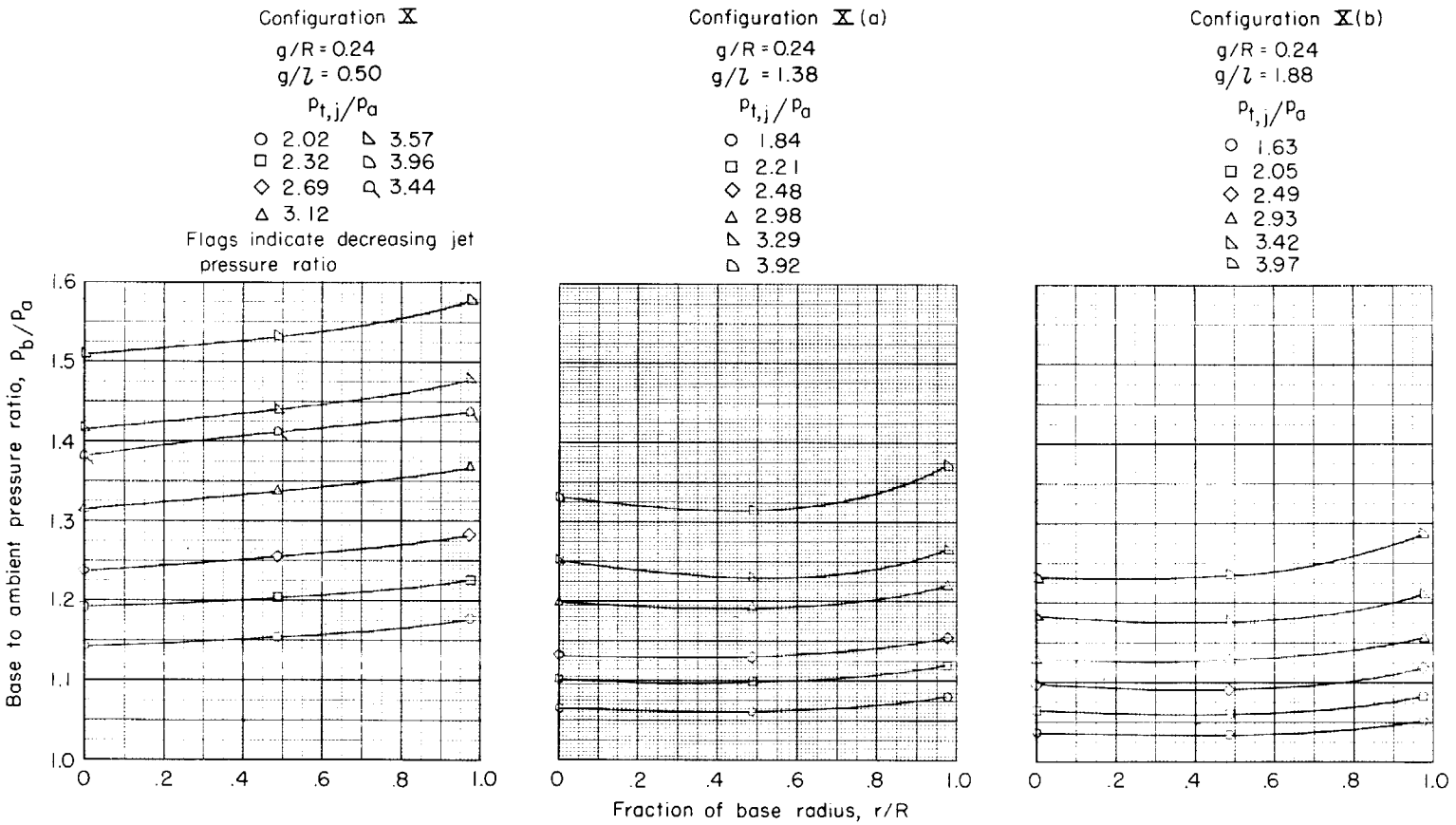

(d) Configuration X.

Figure 6.- Continued.

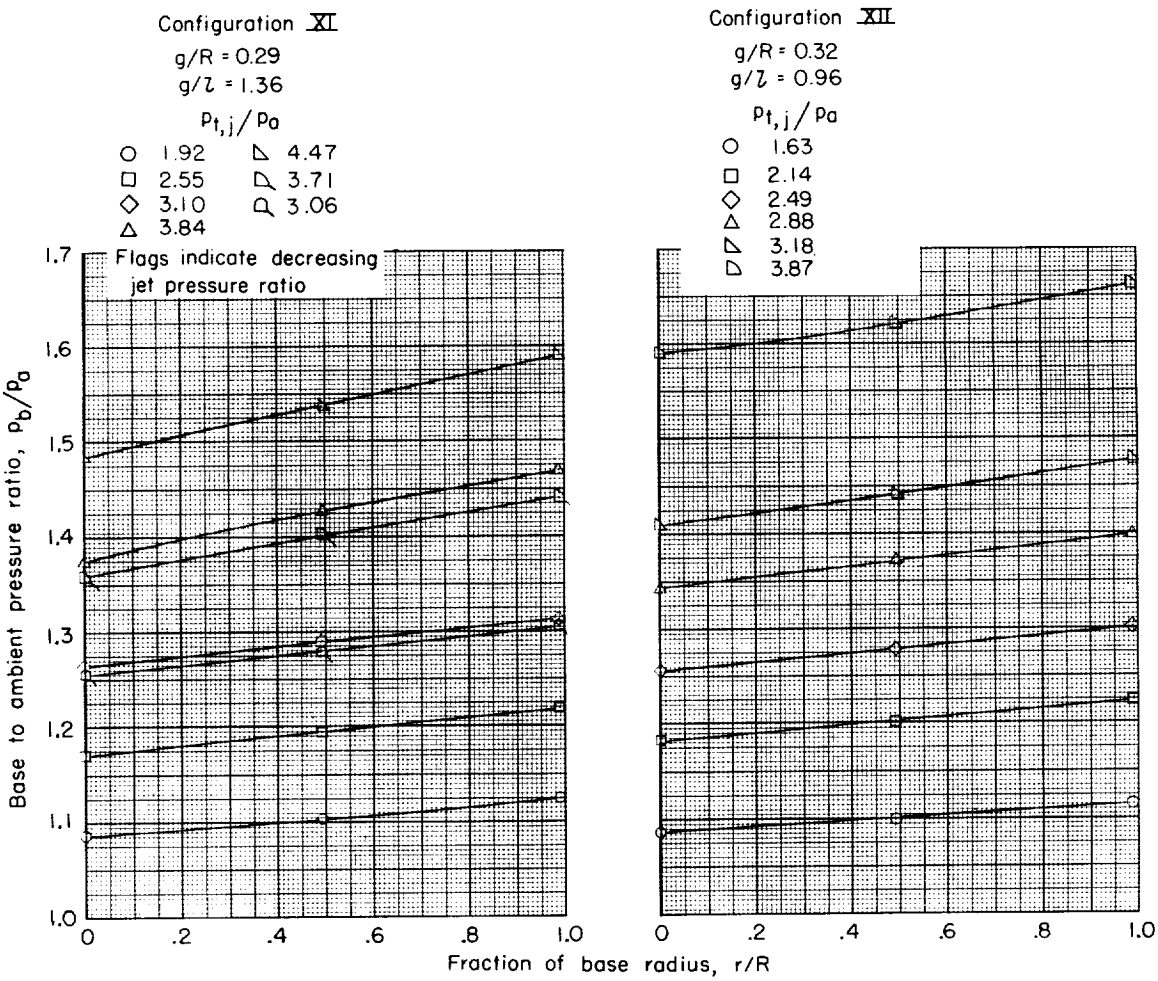

(e) Configurations XI and XII.

Figure 6.- Concluded.

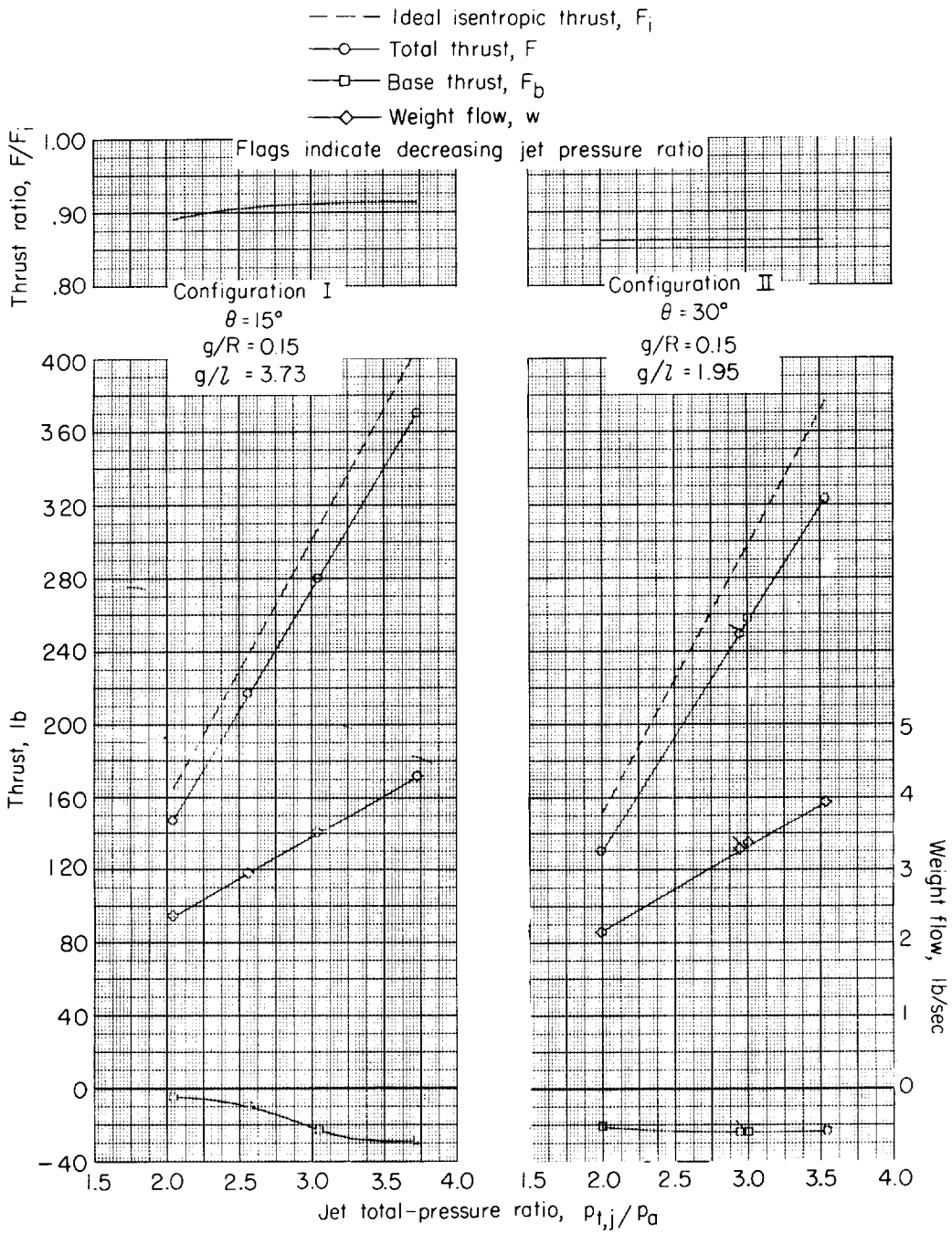

(a) Configurations I and II.

Figure 7.- Variation of nozzle performance with jet total-pressure ratio for series A nozzles.

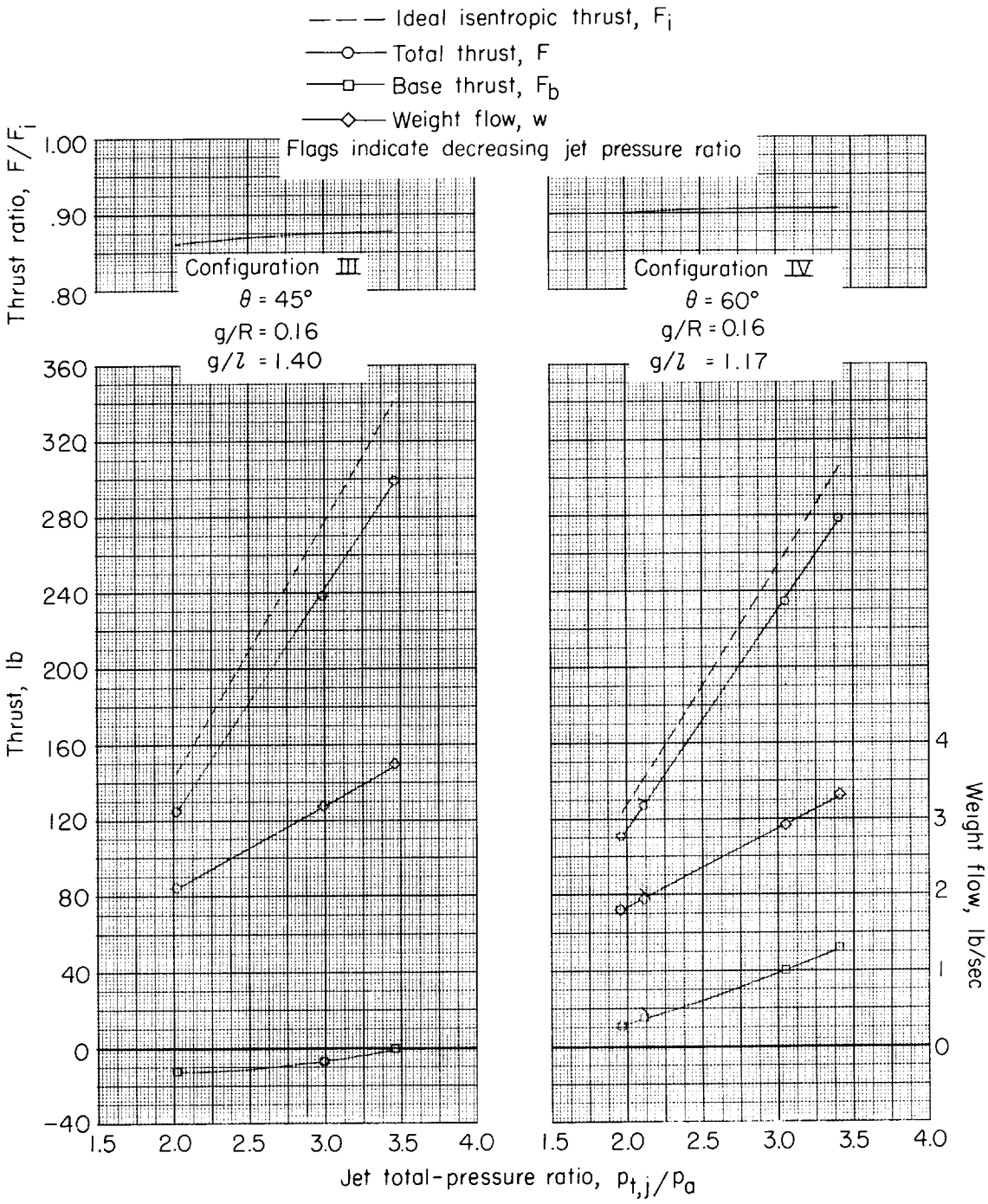

(b) Configurations III and IV.

Figure 7.- Concluded.

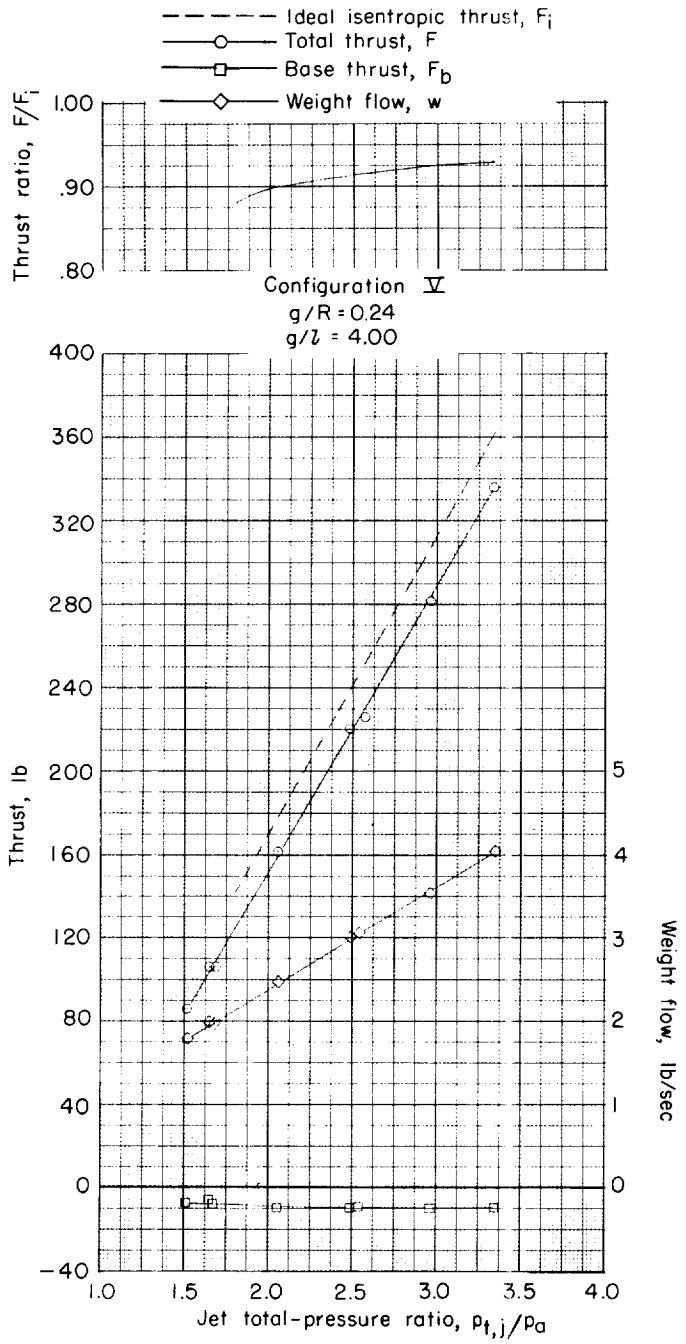

(a) Configuration V.

Figure 8.- Variation of nozzle performance with jet total-pressure ratio for series B nozzles. $\theta = 15^\circ$.

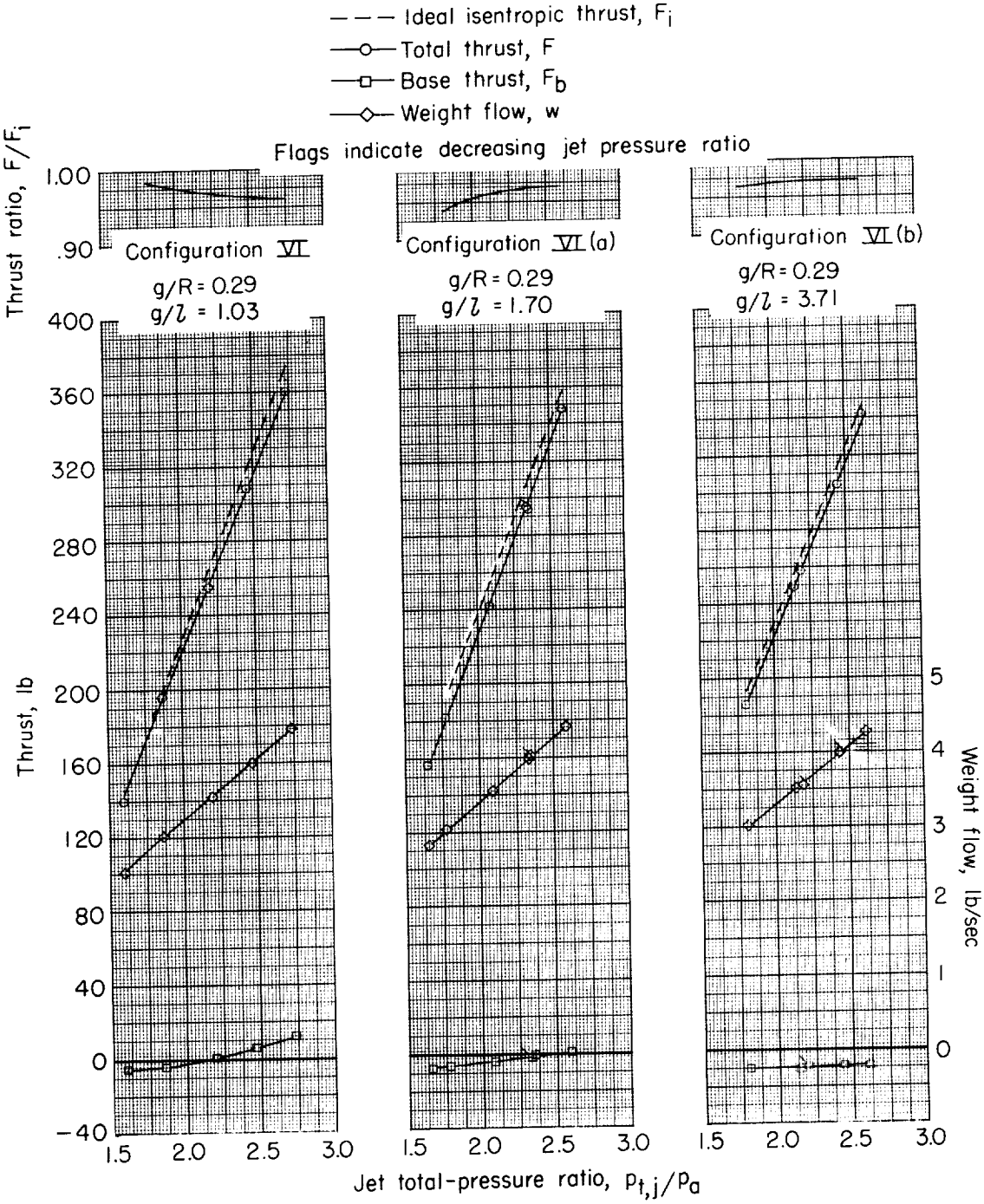

(b) Configuration VI.

Figure 8.- Concluded.

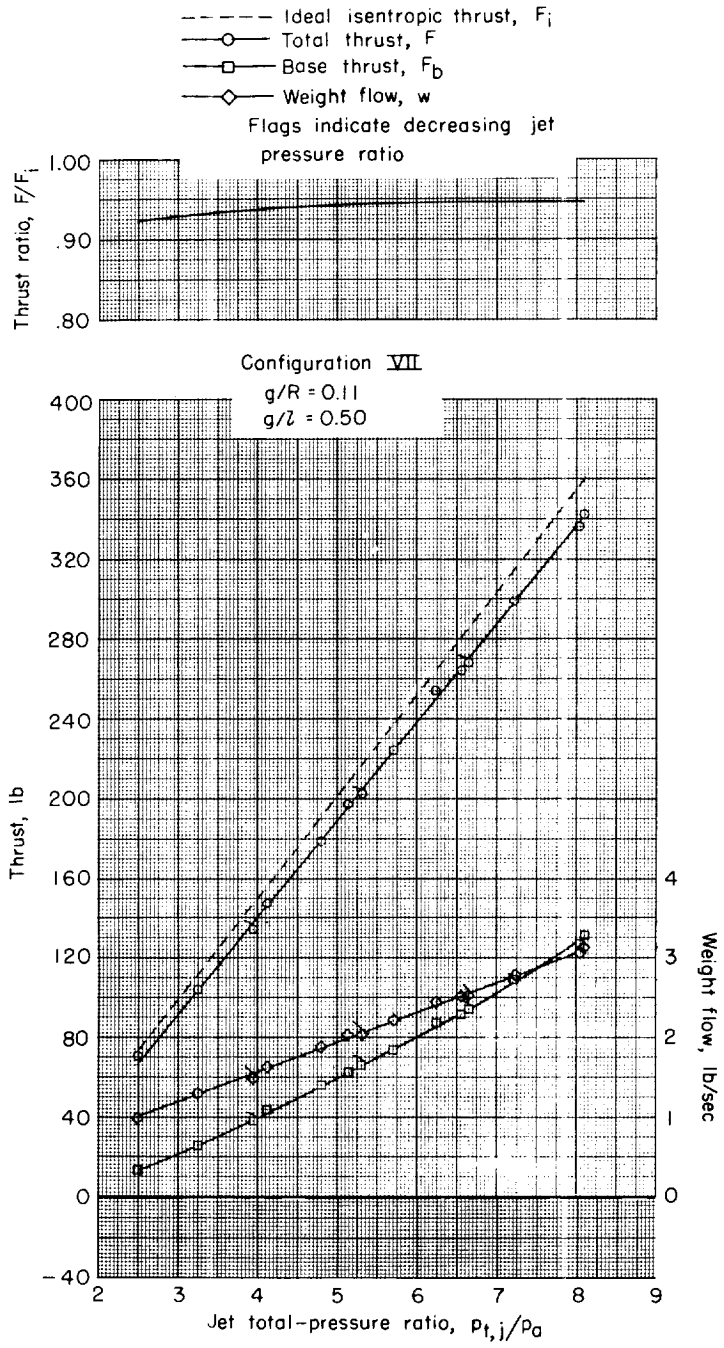

(a) Configuration VII.

Figure 9.- Variation of nozzle performance with jet total-pressure ratio for series C nozzles. $\theta = 30^\circ$.

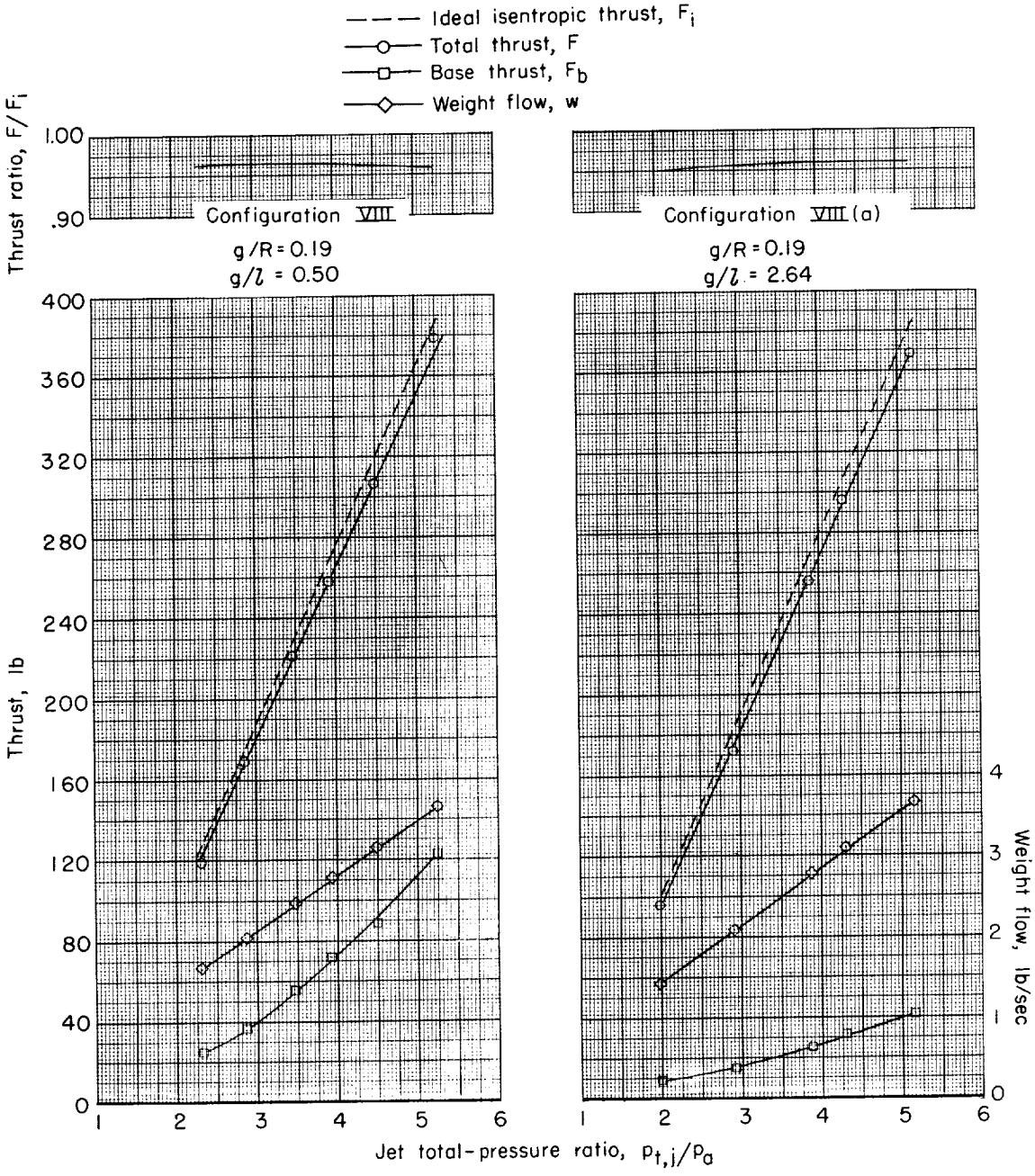

(b) Configuration VIII.

Figure 9.- Continued.

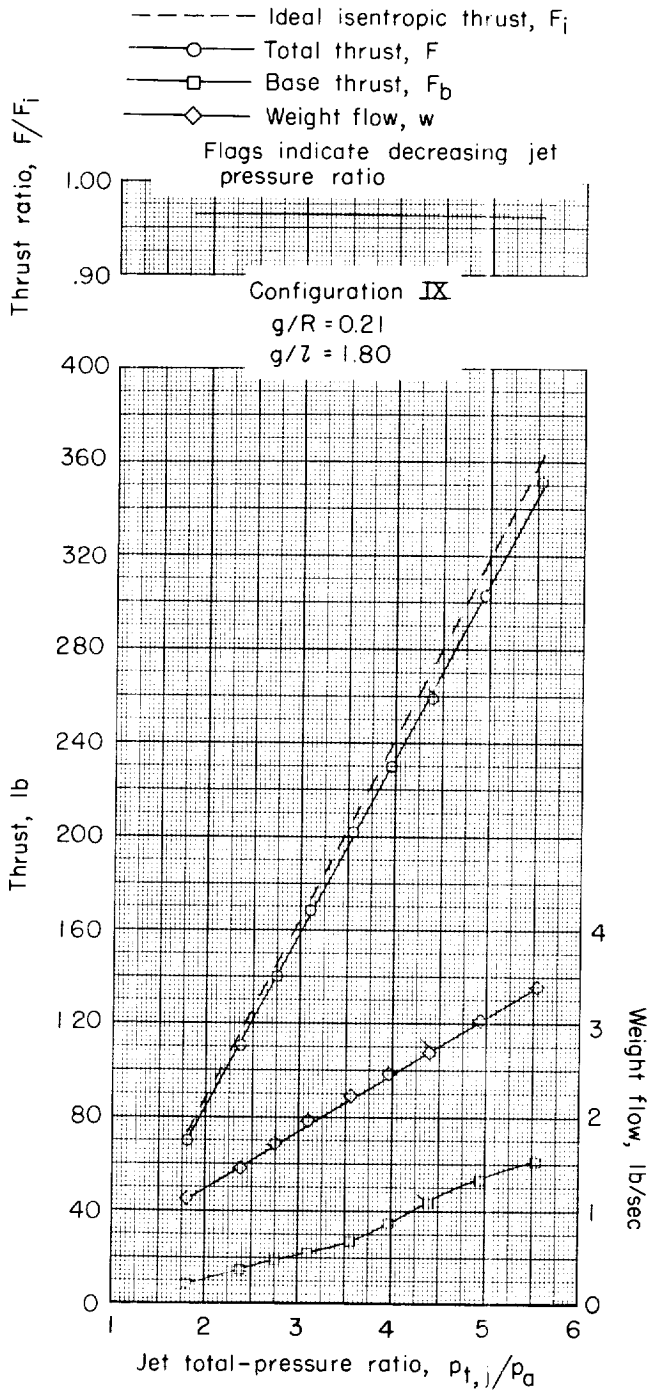

(c) Configuration IX.

Figure 9.- Continued.

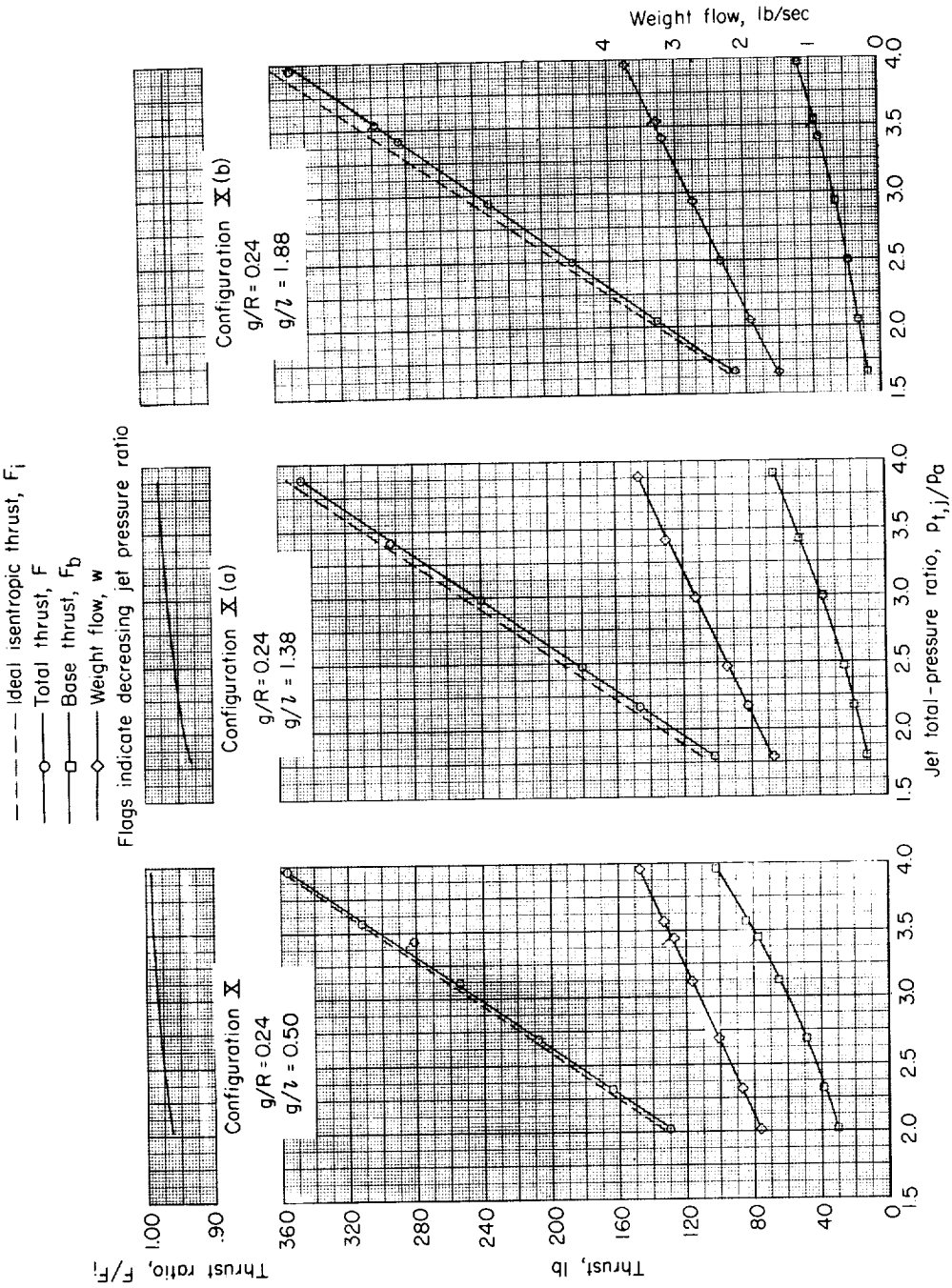

(d) Configuration X.

Figure 9.- Continued.

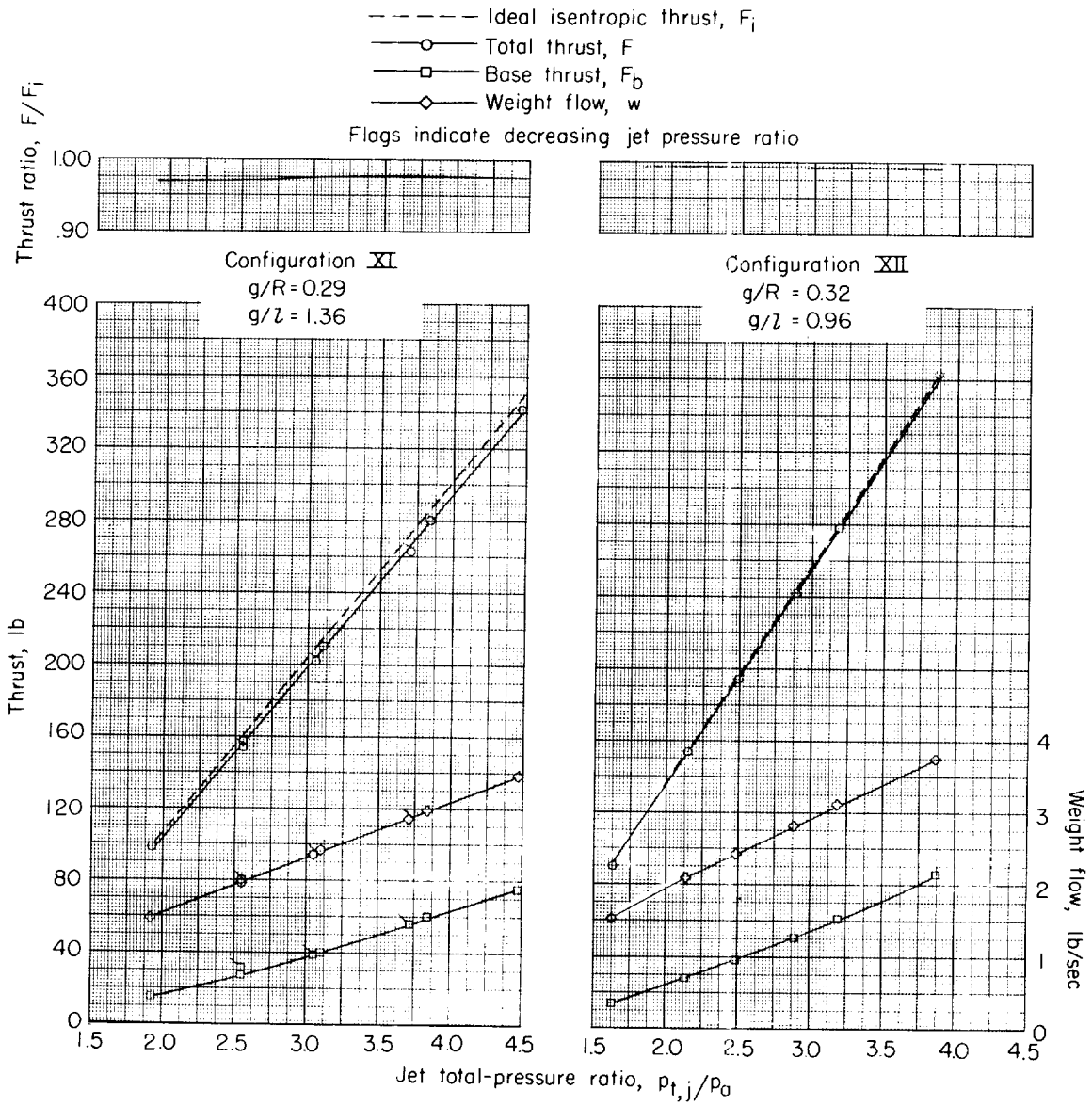

(e) Configurations XI and XII.

Figure 9.- Concluded.

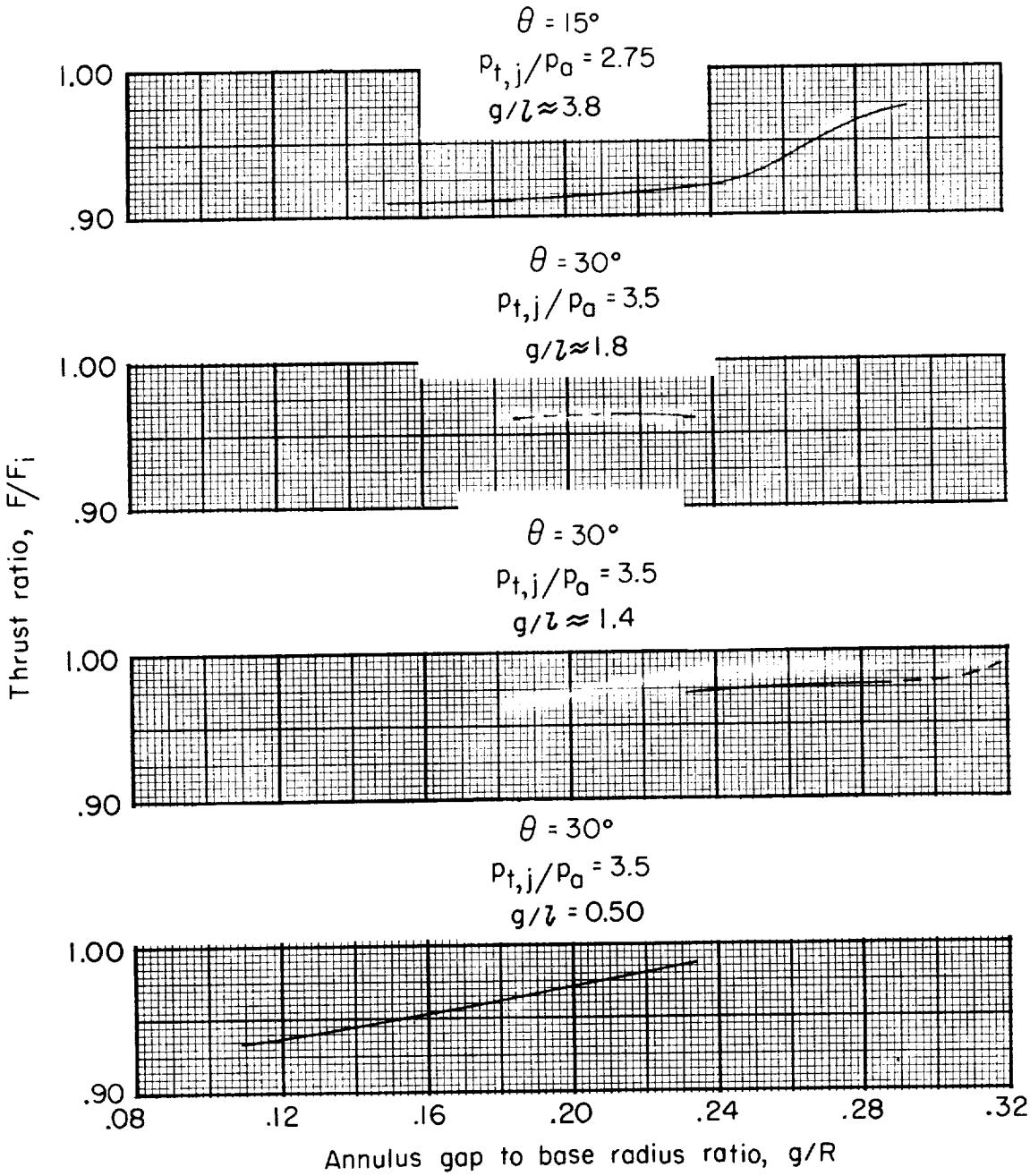

Figure 10.- Effect of annulus gap to base radius ratios on nozzle efficiency for discharge angles of 15° and 30° and for various nozzle lip overhangs.

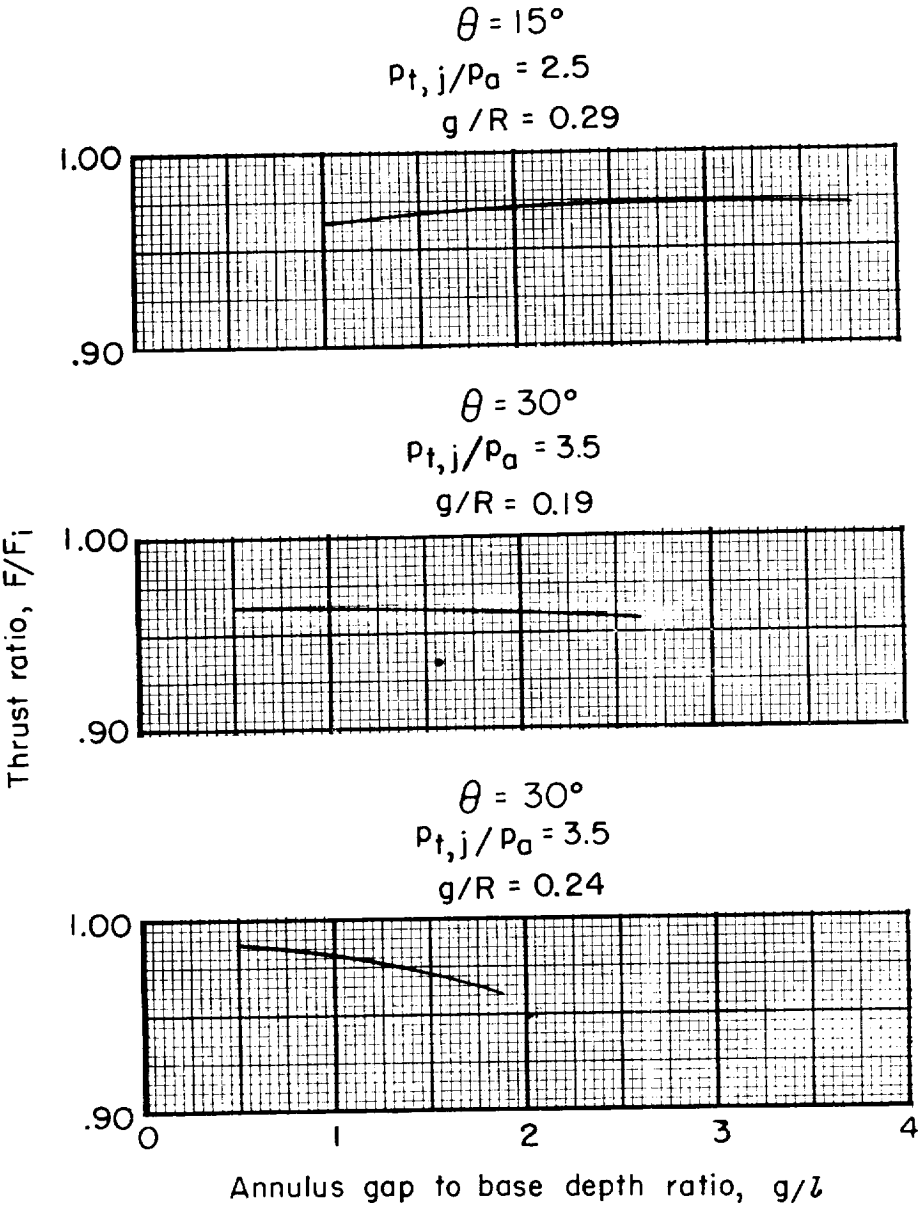

Figure 11.- Effect of annulus gap to base depth ratio on nozzle efficiency for discharge angles of 15° and 30° at constant annular gap to base radius ratios.